Raman scattering study of the phase transition sequence in the $(BA)_{1-x}(DBA)_x$ system

1998 J. Phys.: Condens. Matter 10 6825

(http://iopscience.iop.org/0953-8984/10/30/020)

J. Phys.: Condens. Matter **10** (1998) 6825–6844. Printed in the UK PII: S0953-8984(98)90853-0

Raman scattering study of the phase transition sequence in the $(BA)_{1-x}(DBA)_x$ system

J Agostinho Moreira†, A Almeida†, M R Chaves†, M F Mota†, A Klöpperpieper‡ and Filipa Pinto†

† Departamento de Física, IMAT (núcleo IFIMUP), CFUP, Faculdade de Ciências da Universidade do Porto, Rua do Campo Alegre 687, 4150 Porto, Portugal

‡ Fachbereich Physik, Universität des Saarlandes, 66041 Saarbrücken, Germany

Received 19 January 1998

Abstract. We have measured the polarized Raman spectra of betaine arsenate and deuterated betaine arsenate single crystals in the temperature range 12–300 K. On the basis of the comparative study of Raman spectra of protonated and deuterated compounds and by taking into account the relevant literature data, we proposed a mode assignment for $(BA)_{1-x}(DBA)_x$. The isotopic effect in this system is discussed. The analysis of the internal modes of AsO_4^{3-} clearly shows the important role played by this unit in the phase sequence of $(BA)_{1-x}(DBA)_x$. The strong coupling exhibited by the proton/deuteron modes with the internal modes of AsO_4^{3-} provides some evidence for the ordering of the hydrogen bonds at the phase transitions. In DBA_{92} this analysis reveals the existence of two types of hydrogen bond related to the mechanisms underlying the phase transitions.

1. Introduction

Betaine arsenate, $(CH_3)_3NCH_2COO.H_3AsO_4$, abbreviated to BA, undergoes two phase transitions: a ferrodistortive ferroelastic phase transition at $T_{c1} = 411$ K and a ferroelectric phase transition at $T_{c2} = 119$ K [1, 2]. Above 411 K an orthorhombic $Pbnm$ structure was found [3]. In the ferroelastic–paraelectric phase, BA crystallizes in the space group $P12_1/n1$ with four formula units per unit cell [2]. Below T_{c2}, the space group is $P1n1$ [3, 4] and a spontaneous polarization appears in the plane perpendicular to the screw axis 2_1 with its major component along the c-axis [1]. No doubling of the unit cell is observed in the ferroelectric phase [3, 4]. X-ray studies indicate that the AsO_4^{3-} anions are linked by hydrogen bonds forming quasi-one-dimensional zig-zag chains directed along the c-axis [2]. The betaine molecules are connected to the the AsO_4^{3-} anions by two other hydrogen bonds which are almost perpendicular to the zig-zag chains [2]. Both the tetrahedra and the betaine molecules occupy a general position with no symmetry in the unit cell. The dielectric, pyroelectric, elastic and optical properties of betaine arsenate have been extensively studied [5–10]. The maximum of the anomaly of the dielectric constant at T_{c2} exceeds 5×10^5 and a strong dependence on the frequency and on d.c. electric fields is found [9]. The dielectric behaviour in the low temperature phase has been related to the existence of competitive ferro- and antiferroelectric interactions in this compound [7, 11, 12].

Deuteration changes drastically the phase sequence of BA in the low temperature range but not in the high temperature region: a phase transition from the supposedly high temperature $Pbnm$ phase to the same paraelectric phase with space group $P12_1/n1$ still

takes place at 411 K [11–15]. Yet, for a deuteration content above 77%, an antiferroelectric phase (AFE), with symmetry $P12_11$, appears between the paraelectric (PE) and the ferroelectric phase (FE1). The space group of the FE1 phase is $P1n1$ [4]. The temperature range of stability of the antiferroelectric phase becomes larger when increasing the deuterium content of the crystal. The para–antiferroelectric phase transition is second order and is characterized by a broad maximum of the dielectric constant, smaller than in pure BA ($\approx 5 \times 10^4$) [14]. In the vicinity of this phase transition, a strong frequency dependence of the dielectric constant was observed in the frequency range 100 Hz–10 GHz [16, 17]. The antiferro–ferroelectric phase transition is first order and the ferroelectric phase exhibits an important dielectric dispersion [17]. From dielectric and pyroelectric measurements, an additional first order phase transition to a low temperature polar phase (FE2) with symmetry $P1n1$ was found at 80 K, approximately [14]. The polarization of this phase is much lower than in the FE1 phase.

The phase diagram of the mixed system $(BA)_{1-x}(DBA)_x$ (x, T_c) was obtained through different techniques. Neutron diffraction, ENDOR and EPR measurements [18–20] have shown that the arsenate anion plays a role in the phase transition sequence in these compounds, but a clear explanation of this behaviour has not been given so far.

This work presents a detailed study of polarized Raman spectra as a function of temperature (12–300 K) for different deuterium contents (0%, 58%, 80%, 87% and 92%). The first part concerns the assignment of the vibrational modes of the structural elements of the $(BA)_{1-x}(DBA)_x$ system†. This assignment is based on a comparative study of the Raman spectra of protonated and deuterated compounds and of a compressed powder of betaine. In the second part we present a detailed study of the spectra of some external and internal modes, obtained at different temperatures. One of the main motivations to perform this study was to follow the changes in line widths and in frequencies of the external modes, looking for a better understanding of the order–disorder phase transition displayed by BA and DBA_{92}. Another motivation was to follow the alterations of the internal AsO_4^{3-} modes with temperature in order to obtain evidence for the coupling of the optical modes with the proton and/or deuteron motion. The correlation between the onset of new modes and the breaking of symmetry due to the structural phase transitions or a local disorder will be emphasized. On the basis of this knowledge, we shall show that we obtain a deeper insight of the mechanisms underlying the phase transition sequences of BA and DBA_{92}.

2. Experiment

The single crystals of BA used in our Raman scattering study have been obtained by the aqueous solution method. The deuterated samples have been grown in a solution containing heavy water. The real content of deuterium in the crystals was determined by detecting the transition temperatures through dielectric constant and pyroelectric current measurements [11].

The samples used have the forms of oriented and optically polished parallelepipeds ($3 \times 4 \times 5$ mm^3). As BA and DBA exhibit pseudo-orthorhombic structures (the monoclinic angle is approximately 2°) the faces were cut normal to $x \parallel a$, $y \parallel b$ and $z \parallel c$, within the experimental error. The samples were placed in a closed-cycle helium cryostat (12–300 K temperature range) with temperature stability of about ± 0.2 K. The temperature homogeneity in the samples was achieved with a copper mask set-up.

† From here on, we shall simplify the notation, writing either BA for the protonated sample, or DBA_x for the partially deuterated samples $(BA)_{1-x}(DBA)_x$.

The 514.5 nm (150 mW) line of an Ar^+ laser was chosen for excitation. The scattered light was analysed in the right-angle scattering geometry, using a PC-controlled T64000 Jobin–Yvon triple monochromator, equipped with a CCD camera and a photon-counting device. Identical conditions (laser power, slit width and height, acquisition time) were maintained for all the scattering measurements. The spectral resolution was better than 1.5 cm^{-1}. Along with the measurement of the Stokes Raman spectra, the low frequency anti-Stokes Raman spectra were recorded. This procedure allows for an accurate evaluation of the frequency. The mode parameters were calculated by a least squares fit of the Raman spectra to the response function of damped harmonic oscillators:

$$S(\omega, T) \approx (\omega_L - \omega_o)^4 (n(\omega) + 1) I_0 \Gamma \omega / [(\omega^2 - \omega_o^2)^2 + \Gamma^2 \omega^2] \tag{1}$$

with $n(\omega) = 1/(e^{\hbar\omega/kT} - 1)$, ω_L frequency of the incident radiation, ω_o eigenfrequency of the oscillator, Γ damping constant and I_0 intensity parameter. The intensity is given by:

$$I_0 = \int S(\omega, T)/(n(\omega) + 1)\, d\omega. \tag{2}$$

3. Experimental results at room temperature

In this section, we describe our Raman spectra obtained with samples cut in different geometries, in the 4 cm^{-1}–3500 cm^{-1} frequency range and we try to identify their origins. Figure 1 shows the Raman spectra corresponding to the six components of the polarizability tensor of BA in the 15 cm^{-1}–3100 cm^{-1} frequency range at room temperature.

The $2/m$ factor group comprises four symmetry types: two are Raman active ($A_g(xx, yy, zz, xz)$ and $B_g(xy, yz)$) and two are infrared active ($A_u(y)$ and $B_u(x, z)$). The 321 optical phonon modes of BA have to be assigned as 78 A_g, 78 B_g, 83 A_u and 82 B_u. The identification of some of these modes was obtained through a comparative study of Raman spectra of protonated and deuterated samples. In this analysis we have also taken into account the relevant information referred to in current literature. The replacement of a hydrogen atom by a deuterium atom changes the frequencies and profiles of the normal modes due to two different effects: a direct effect due to the difference of masses and a geometrical effect originating in changes of the length and of the angles of the molecular units. A breaking of selection rules resulting from the local disorder due to the random distribution of deuterium atoms is expected. This disorder can change also the mode coupling strength and, consequently, alter the resonance phenomena.

3.1. External modes

In the analysis carried out in this paragraph, we assume that each unit cell is formed by eight rigid units: four arsenate anions and four betaine molecules linked by hydrogen bonds. As can be seen in figure 2, these bonds are O_1–$H_{14}\cdots O_5$, O_2–$H_{12}\cdots O_3$, O_6–$H_{15}\cdots O_6$ and O_4–$H_{13}\cdots O_4$. The first three are oriented mainly along the *a*-axis and the last one mainly along the *c*-axis. The external modes associated with these units are found to be below 250 cm^{-1}.

The spectra of BA, DBA_{58} and DBA_{92} in the 15 cm^{-1}–200 cm^{-1} frequency range are shown in figures 3(a) to 3(f). In all the scattering geometries and for all the deuterium contents, we can observe some bands below 120 cm^{-1} which correspond to translation and libration collective modes involving the arsenate anion and the betaine molecule. Below 50 cm^{-1}, we notice important differences between the spectra of the protonated and the

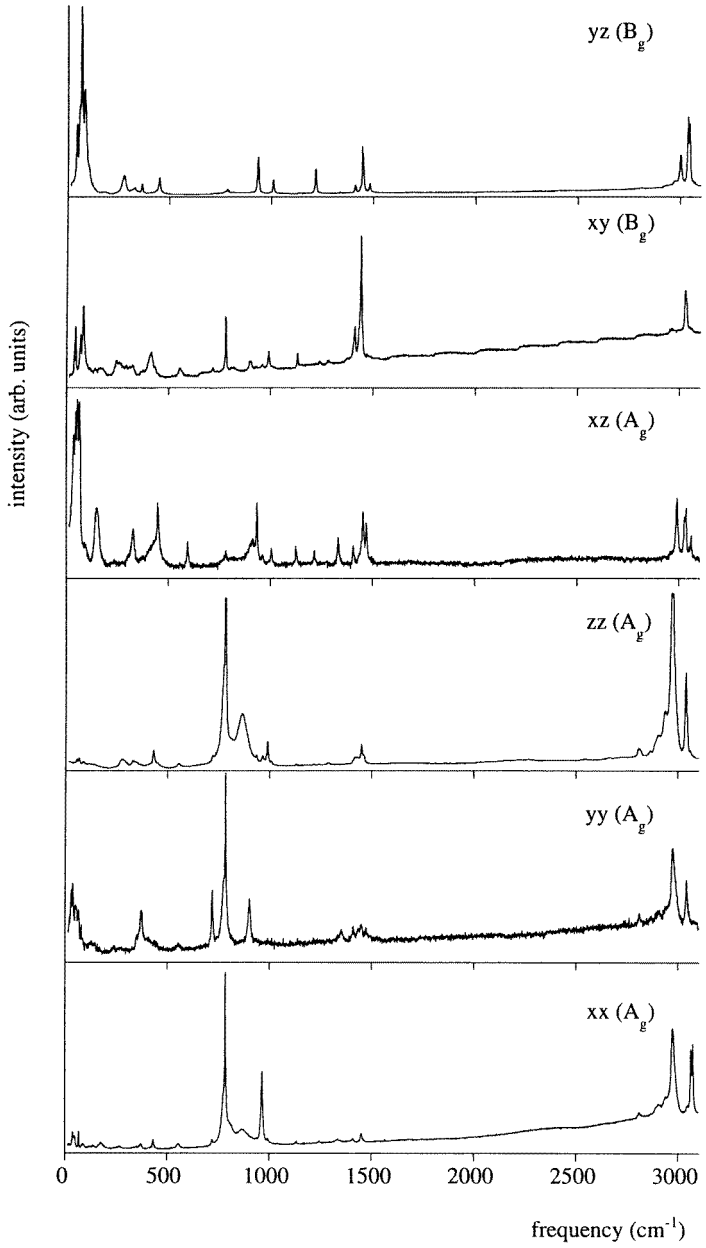

Figure 1. The polarized Raman spectra of BA at room temperature.

deuterated systems in the xx and yy orientations, while no differences or very small ones are found for the other four geometries. This behaviour is presumably related to a change of the lattice parameters with deuteration, which determines changes of the frequency of the external modes. According to [21], the bending γO···O (out-of-plane) and δO···O (in-plane) bands and the stretching bands νO···O are located in the frequency range 80 cm^{-1}–200 cm^{-1}. Making use of this information, we have tentatively assigned the band at 84 cm^{-1}

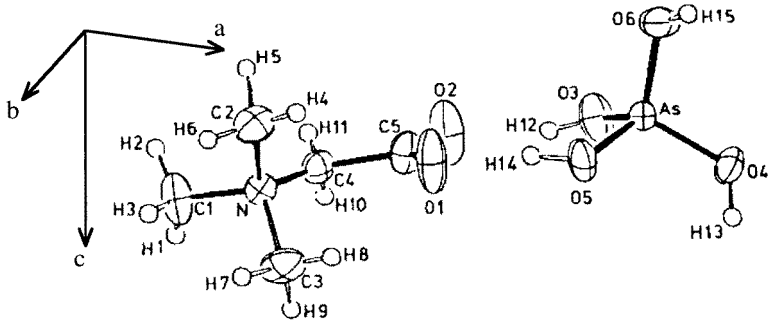

Figure 2. ORTEP plot of the unit formula of BA [2].

to the $\gamma O\cdots O$ mode and the band at 150 cm^{-1} to the $\delta O\cdots O$ mode. If this assignment is correct, this means that the deuteration does not change significantly the $O\cdots O$ band frequencies of the protonated compound. These bands are mainly visible in xx, zz and xz geometries, which is consistent with the orientation of hydrogen bonds referred above.

3.2. Internal modes

Let us now address the problem of identifying the internal vibration modes of the arsenate anion, the hydrogen bonds and the betaine molecule.

3.2.1. Internal modes of the AsO_4^{3-} *anion.* The free arsenate anion, AsO_4^{3-}, with $\bar{4}3m$ symmetry, has four normal modes, all Raman active: the non-degenerate and totally symmetrical stretching mode ν_1, the two degenerate bending modes ν_2, the three degenerate stretching modes ν_3 and the three degenerate bending modes ν_4. The numerical values reported in the literature for the frequencies of these modes are $\nu_1 \approx 837$ cm^{-1}, $\nu_2 \approx 349$ cm^{-1}, $\nu_3 \approx 878$ cm^{-1} and $\nu_4 \approx 463$ cm^{-1} [22].

In some compounds containing the tetrahedral units AsO_4^{3-} or PO_4^{3-} as well as in some organic or inorganic groups, the identity of these anions is maintained. Such an effect is observed when all the hydrogen bonds which link the ion to the rest of the crystal have a similar strength. More frequently, the influence of a less symmetrical environment lifts the degeneracy of the modes. This kind of behaviour is found in a large number of systems such as the KDP family. Since the site group of the anions in $(BA)_{1-x}(DBA)_x$ system is 1, one expects a total lifting of this degeneracy so that the nine internal modes of the AsO_4^{3-} will become visible in each of the four symmetries species of $P12_1/n1$.

We present below a tentative assignment of the vibrational modes of AsO_4^{3-} for BA as well as for DBA_{92} based on the fact that the internal modes of the betaine molecule chain (C_3N–C–C) are expected to be little affected by the crystal field.

By taking into account the numerical values of the ν_1 and ν_3 modes of the free AsO_4^{3-}, we have looked for the corresponding values in the frequency range 700 cm^{-1}–900 cm^{-1} for BA and DBA_{92} single crystals. Figures 4(a), (b) and (c) show the spectra of a betaine compressed powder, as well as those of BA and of DBA_{92} for the A_g symmetry, in that frequency range. On all these figures, a band is found at 785 cm^{-1} which may be attributed to the symmetrical stretching mode of C_3N in the betaine compressed powder. Since in the 770 cm^{-1}–790 cm^{-1} region, the deuterated compound presents two bands, one at

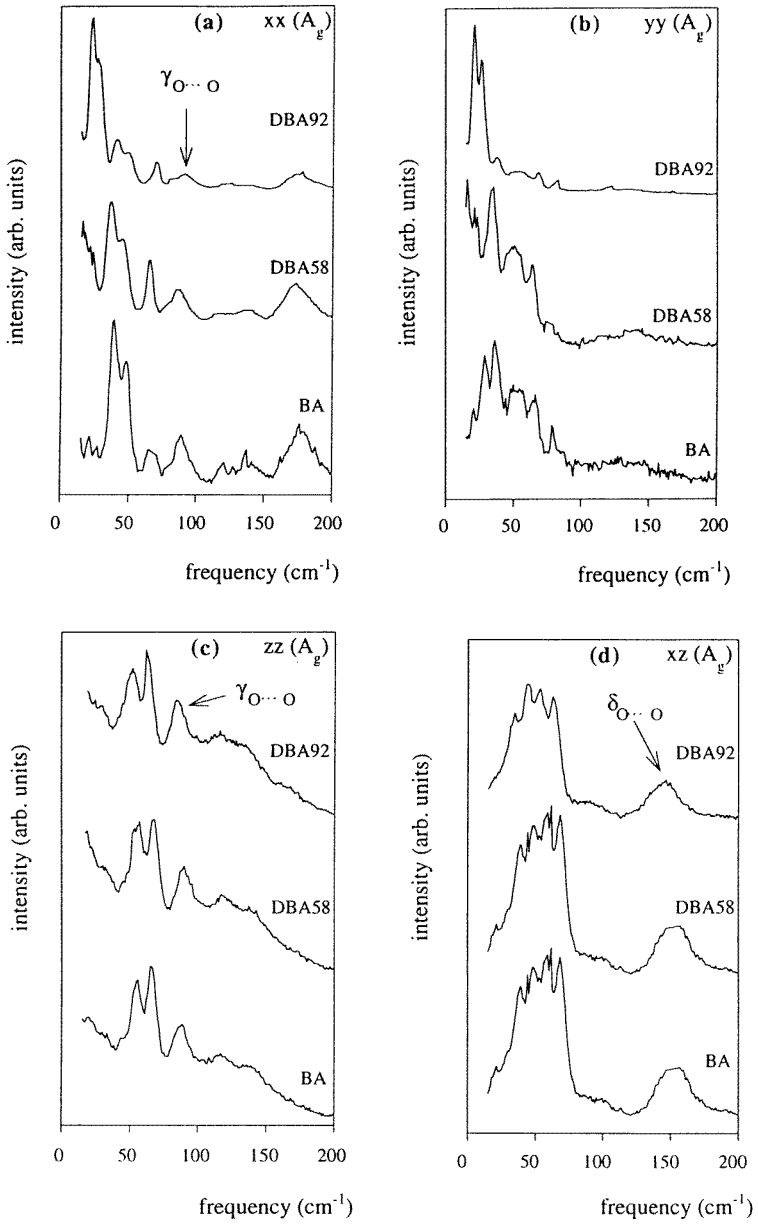

Figure 3. The Raman spectra of BA, DBA_{58} and DBA_{92} in the external mode region for the geometries: (a) *xx*, (b) *yy*, (c) *zz*, (d) *xz*, (e) *xy* and (f) *yz*.

approximately the same frequency, 785 cm^{-1}, and the other one at a lower frequency, 770 cm^{-1}, we assign the 785 cm^{-1} band to $\nu_s C_3N$ and the other one to the ν_1 mode, while we propose that for BA, the ν_1 frequency is also 785 cm^{-1}, overlapping with the $\nu_s C_3N$ band. In figures 4(b) and (c) we also observe, in the 700–900 cm^{-1} region, three additional bands at $\nu_{3a} = 776$ cm^{-1}, $\nu_{3b} = 810$ cm^{-1} and $\nu_{3c} = 865$ cm^{-1} in BA, which shift to 761 cm^{-1}, 792 cm^{-1} and 872 cm^{-1} in DBA_{92}, respectively. By taking into account the

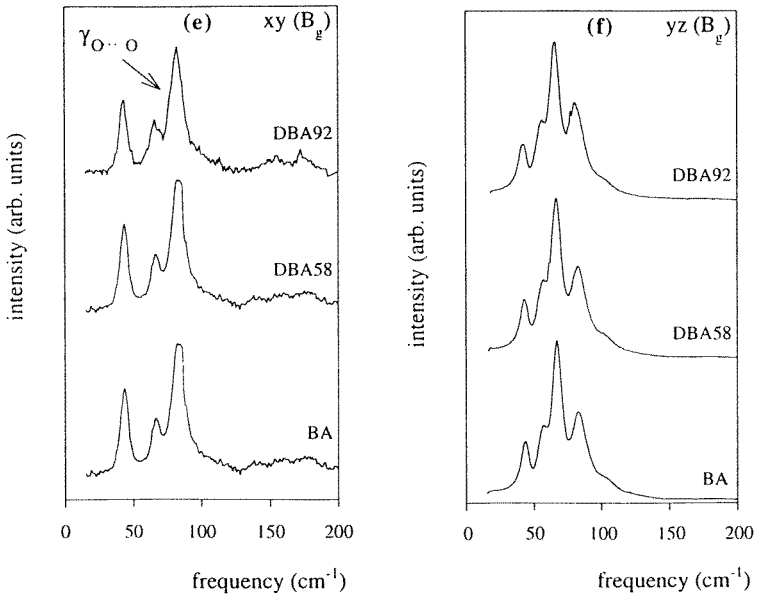

Figure 3. (Continued)

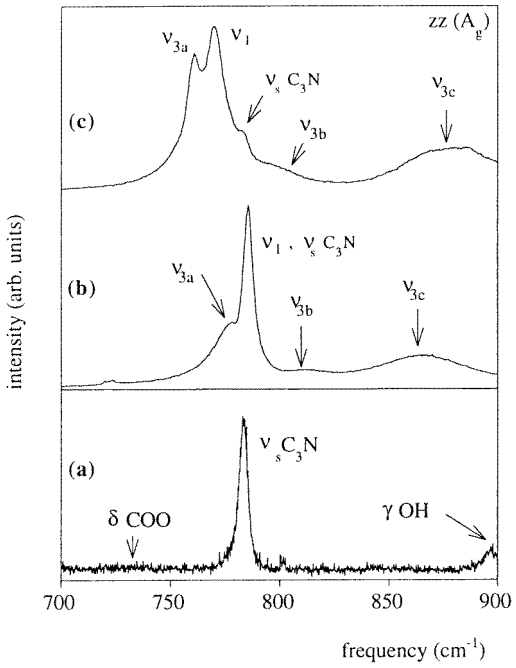

Figure 4. The Raman spectra of (a) betaine compressed powder, (b) BA and (c) DBA_{92} in the frequency range 700 cm^{-1}–900 cm^{-1}.

characteristic broad profile of these bands and their frequency dependence on deuteration, we have identified them as the three non-symmetrical stretching modes of the arsenate anion.

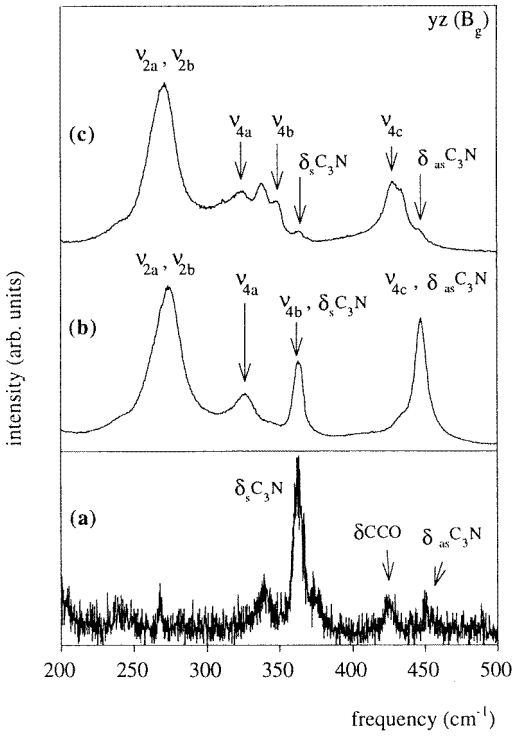

Figure 5. The Raman spectra of: (a) betaine compressed powder, (b) BA and (c) DBA_{92} in the frequency range 200 cm^{-1}–500 cm^{-1}.

In figures 5(a), (b) and (c) are shown the spectra of a betaine compressed powder, and those of BA and of DBA_{92} single crystals for the B_g symmetry in the 200 cm^{-1}–500 cm^{-1} frequency range. In all these spectra, two bands are observed at 362 cm^{-1} and 450 cm^{-1} which are related to the vibration modes $\delta_s C_3N$ and $\delta_{as} C_3N$ of the betaine molecule, respectively. In the deuterated compound, each of these bands splits into two bands: two of these bands remain at the same frequency, i.e. 362 cm^{-1} and 450 cm^{-1} while the two others appear at 346 cm^{-1} and 427 cm^{-1}, respectively. As for the ν_1 mode, we propose that this effect results from an accidental degeneracy, in BA, between two of the non-degenerate ν_{4b} and ν_{4c} modes of the AsO_4^{3-} ion with the $\delta_s C_3N$ and $\delta_{as} C_3N$ modes of the betaine. This degeneracy does not persist in DBA_{92}, whence the shift from 362 cm^{-1} to 346 cm^{-1} and from 459 cm^{-1} to 427 cm^{-1} of these modes. The remaining non-symmetrical bending mode ν_{4a} of the arsenate anion is found at 326 cm^{-1} in BA, and shifts to 323 cm^{-1} in DBA_{92}. An argument for the degeneracy between the C_3N and the ν_4 modes in BA can be found in the fact that the ν_4-type bands present a fairly high intensity that can be explained by means of a charge transfer mechanism coupling the C_3N and the ν_4-type modes. This mechanism may be related to the permanent dipole moment of the betaine molecule. By assuming that deuteration weakens the coupling between the arsenate anion and the betaine molecule modes, a decrease of the intensity in DBA_{92} may occur. The broad and intense band at 273 cm^{-1} in BA is assigned to the symmetrical bending modes ν_{2a} and ν_{2b}. The best fit to expression (1) gives, for these modes, the frequencies 269 cm^{-1} and 276 cm^{-1},

which are shifted in DBA_{92} to 264 cm^{-1} and 271 cm^{-1}, respectively. According to this analysis we list in table 1 a mode assignment for the internal modes of arsenate anion for BA as well as for DBA_{92}.

Table 1. Frequencies of the internal modes of the free arsenate anion and of AsO_4^{3-} in BA and in DBA_{92}.

	ν_1 (cm^{-1})	ν_2 (cm^{-1})		ν_3 (cm^{-1})			ν_4 (cm^{-1})		
Free anion	837	349		878			463		
BA	785	269	276	776	810	865	326	362	450
DBA_{92}	770	264	271	761	792	872	323	346	427

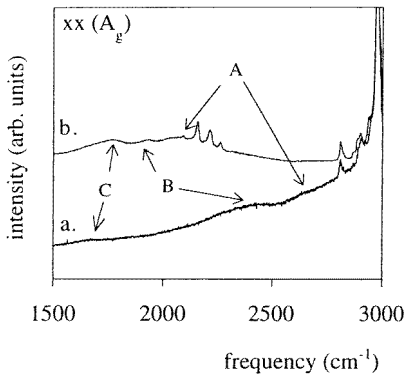

Figure 6. The Raman spectra of (a) BA (xx geometry) and (b) DBA_{92} (xx geometry) in the region of stretching modes of the hydrogen bonds.

3.2.2. Internal modes related to the hydrogen bonds. Let us now turn to the behaviour of the stretching modes (νOH) and of the bending modes (in-plane, δOH, and out-of-plane, γOH) of the hydrogen bonds.

The frequency of the stretching modes is strongly dependent on the O···O length, as is found in the KDP family, $RbHSO_4$, $KH_3(SeO_3)_2$, TGS etc [23]. This feature can be used to evaluate the hydrogen bond strength. If the O···O length is larger than about 2.7 Å, the bonding is weak, the H atom is mainly attached to one oxygen and a narrow band ($\Delta_{1/2} < 50$ cm^{-1}) appears around 3200 cm^{-1} [24, 25]. For lengths between 2.6 Å and 2.7 Å the bonding increases, the H atom starts to be linked to two oxygen atoms and broader bands are found in the frequency range 2800 cm^{-1}–3100 cm^{-1}. Finally when the O···O length still decreases to be between 2.45 Å and 2.6 Å, the hydrogen bonds are strong and three broad bands, labelled A, B and C bands, are exhibited in the frequency range 1500 cm^{-1}–2800 cm^{-1} [24, 25]. The behaviour of the bending modes is more complex and no simple relationship between the O···O distance and the frequencies can be found. One simply knows that the δOH and γOH modes are usually found between 1240 cm^{-1} and 1350 cm^{-1} and between 900 cm^{-1} and 1000 cm^{-1}, respectively.

The isotopic ratio ($r = f_{OH}/f_{OD}$) has values which depend on the type of mode. r is less than 1.40 for the stretching modes, is between 1.40 and 1.45 for the δ bending modes and is larger than 1.45 for the γ bending modes [26].

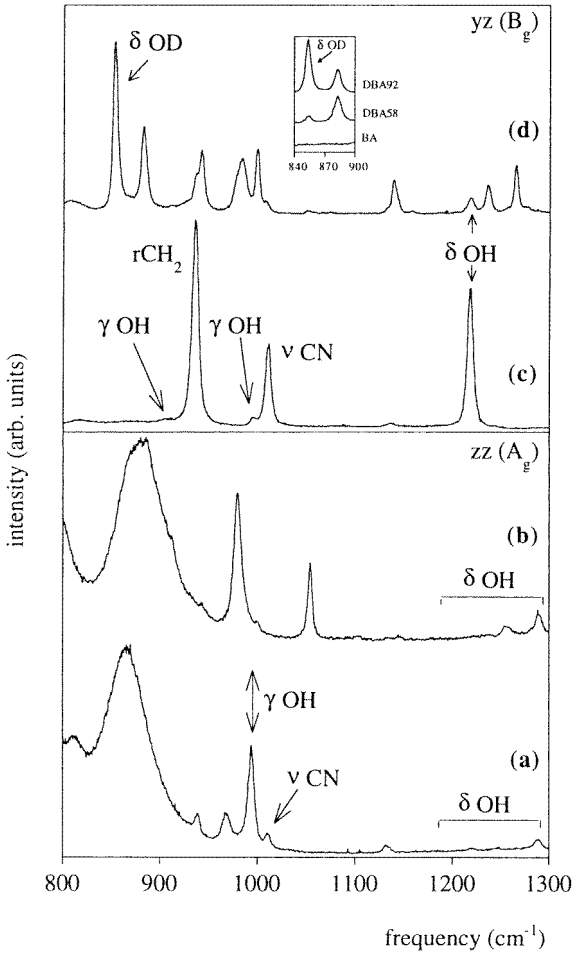

Figure 7. The Raman spectra of (a) BA (zz geometry) and (b) DBA_{92} (zz geometry) and (c) BA (yz geometry) and (d) DBA_{92} (yz geometry) in the frequency range 800 cm^{-1}–1300 cm^{-1}.

On the basis of these results, we have identified the three broad bands centred at 2664 cm^{-1}, at 2417 cm^{-1} and at 1694 cm^{-1} in the xx geometry spectra of the BA samples with the A, B and C bands (see figure 6(a)). The numerical values are consistent with the existence of strong hydrogen bonds in the protonated system. In the zz geometry, these bands are less visible. Deuteration shifts and compresses the bands, which are now found centred at 2082 cm^{-1}, at 1932 cm^{-1} and at 1774 cm^{-1} in DBA_{92} (figure 6(b)).

Figure 7 shows the Raman spectra of BA and DBA_{92} obtained at room temperature for the zz and yz geometries in the region expected for the γOH and δOH modes. In the last geometry (figure 7(c)) we see a sharp and intense peak at 1217 cm^{-1} in the protonated compound and a much smaller peak in DBA_{92} spectra (figure 7(d)). Two sharp peaks at 853 cm^{-1} and at 875 cm^{-1} arise in the spectra of the deuterated compound. As, in this frequency range, no bands are found for BA, one of them can be related very likely to the bending mode δOD. Since the intensity of the peak at 853 cm^{-1} is strongly dependent on the deuterium content while the intensity of the peak at 875 cm^{-1} remains practically

constant in all deuterated samples (see inset of figure 7) we have associated the former to the δOD mode. The 875 cm^{-1} peak may be due to a local breaking of symmetry. With such an assignment, the isotopic ratio is 1.43, consistent with the values referred above for the δ-bending modes. The broad band visible in zz geometry between 1230 and 1300 cm^{-1} is assigned to the other δOH bending modes (figures 7(a) and (b)). We have identified tentatively the very weak bands at 990 cm^{-1} and 900 cm^{-1} to the bending modes γOH (figures 7(a), (b) and (c)). The bending modes γOD are not found in the frequency range 600–700 cm^{-1}, where they could have been expected, which is probably due to their very small intensity. The several γOH and δOH bands that we have found give evidence for the existence of different types of hydrogen bond.

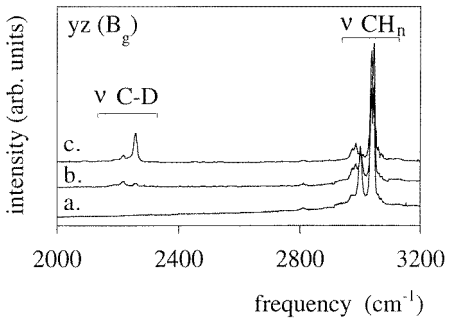

Figure 8. The Raman spectra of (a) BA, (b) DBA_{58} and (c) DBA_{92} in the frequency range 2000 cm^{-1}–3200 cm^{-1}.

3.2.3. Internal modes of the betaine molecules. Table 2 indicates the frequencies of the internal modes of the betaine molecule in BA. They were obtained from the comparison of BA, DBA_{92} and betaine compressed sample spectra and by taking into account the literature data [27]. Figure 8 shows the Raman spectrum of those systems at room temperature, in the yz scattering geometry, between 2000 cm^{-1} and 3200 cm^{-1}. We found an isotopic ratio approximately equal to $\sqrt{2}$ between the frequencies of the 3086 cm^{-1}, 3042 cm^{-1} and 2946 cm^{-1} bands in BA and the 2182 cm^{-1}, 2150 cm^{-1} and 2083 cm^{-1} bands in DBA_{92} spectra, respectively. We can thus identify the first three bands with the stretching modes of C–H groups and the last three to the stretching modes of C–D groups. These results show that not only the protons of the inorganic tetrahedra are substituted by deuterium, but that also the protons of the betaine molecule are partially substituted by deuterons.

4. Phase transition sequence

4.1. Phase transition sequence in BA

The phase transition at 411 K can be described as the condensation of a zone centre B_{2g} mode of the high temperature structure related to the rotation of the betaine molecules around the monoclinic b-axis. The transition from the paraelectric–ferroelastic phase to the ferroelectric phase at 119 K is associated with a polar B_u mode of $P12_1/n1$ at $\boldsymbol{k} = 0$. Since the components x and z belong to the basis of the B_u representation, a spontaneous polarization in the ac-plane is expected. The study of some features of the order parameter should be then accomplished by recording the A_g low frequency spectra (diffusion geometry xx, yy or zz) as a function of the temperature.

Table 2. List of the betaine internal modes in BA.

Frequency (cm^{-1})	Assignment
3086	νC–H
3004	νCH_3
3042	νC–H
2975	νCH_3
2946	νC–H
2884	νCH_3
2810	νCH_3
1462	$\delta_{as} CH_3$
1450	$\delta_{as} CH_3$
1411	ν_sCOO
1344	ν_sCOO
1335	ωCH_2
1244	tCH_2
1130	rCH_2
1005	νCN
986	$\nu_{as} C_3N$
966	νCC
932	rCH_2
784	$\nu_s C_3N$
720	δCOO
450	$\delta_{as} C_3N$
435	δCCO
362	$\delta_s C_3N$

The external A_g modes in the zz geometry can be seen in figure 9(a). On lowering the temperature, some lines become better resolved as a result of a natural decrease of their widths, which indicates a lowering of the anharmonicity of the thermal vibrations. New peaks around 65, 150 and 160 cm^{-1} reveal the signature of the structural transformation that occurs at T_{c2}, but there is no evidence for the existence of a soft mode indicative of a displacive phase transition at this temperature, in agreement with [6]. There are also no clear hints of an order–disorder phase transition, since no explicit changes in the half-widths of the bands are visible and the central peak does not display significative wings (see inset in figure 9(a)). So the low frequency A_g spectrum does not give a clear indication about the character of the phase transition of betaine arsenate at T_{c2}. The frequency of the peaks whose maxima are at 53 cm^{-1} and 64 cm^{-1} at 295 K increases slightly as the temperature decreases. This feature may be related to the behaviour of the order parameter of the para–ferroelastic phase transition at 411 K.

As concerns the behaviour of the internal modes, the most interesting features are related to the AsO_4^{3-} ions. The spectra of these modes and the temperature dependence of their frequencies are displayed in figures 9(b), (c) and 10, respectively.

The bending modes ν_2, due to their torsional character, are known to be very sensitive to proton or deuteron ordering [29]. This is in agreement with figure 10, where we see a clear change of the slope of $\nu_{2a}(T)$ and $\nu_{2b}(T)$ at $T_{c2} = 119$ K. The dashed curves in that figure are qualitative extrapolations for $T < T_{c2}$ of the expected Debye lattice-anharmonic contributions. We observe that the experimental data $\nu_{2b}(T)$ are shifted downwards, relatively to the corresponding dashed curve. In fact, if the protons become ordered, they attach to the AsO_4^{3-} ions and this vibrating unit becomes more massive, hence a lowering of its frequency must occur. The behaviour of the $\nu_{2b}(T)$ agrees with

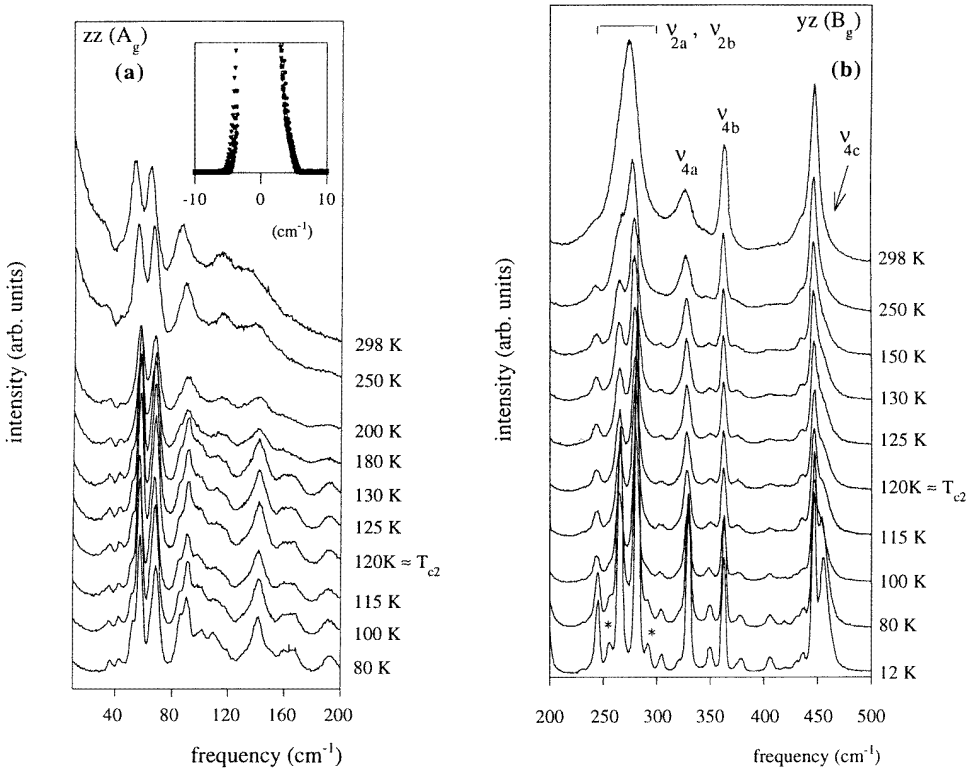

Figure 9. The Raman spectra for BA for different temperatures in the frequency range: (a) 5 cm^{-1}–200 cm^{-1}; (b) 200 cm^{-1}–500 cm^{-1}; (c) 700 cm^{-1}–900 cm^{-1}; (d) 1150 cm^{-1}–1350 cm^{-1}.

this prediction: below T_{c2}, the $\nu_{2b}(T)$ mode frequency is lower than its extrapolated high temperature value. Yet, though the $\nu_{2a}(T)$ mode also changes its slope near T_{c2}, the shift is smaller and in the opposite direction. The explanation of this effect requires a more complex mechanism; the latter may be related to a change of the coupling strength between the AsO_4^{3-} ion and the betaine molecule, through dipole interactions, enhanced by the proton ordering. This assumption is supported by the anomaly observed in the frequency of the δCCO mode (see figure 10).

As is well known, the breaking of symmetry which takes place at a structural phase transition is always followed by the onset of new Raman modes. The intensity of these new modes must be proportional to the square of the order parameter. Since the yz geometry is particularly sensitive to the breaking of symmetry that takes place at T_{c2}, we have analysed the temperature dependence of the intensity of the ν_2 A_u modes (see figure 9(b)). In the inset of the figure 10 we can see that the plots of the intensity of the new bands versus temperature follow the expected linear behaviour, in agreement with a Landau theory of a displacive character. Yet, the same effect does not show up clearly for the other internal modes of the AsO_4^{3-} ion. We can discuss, below, only the changes of frequency of these modes.

Among the bending ν_4-type modes, only ν_{4c} presents some signature of the onset of the ferroelectric phase. The behaviour of the ν_3 modes is difficult to interpret: their temperature

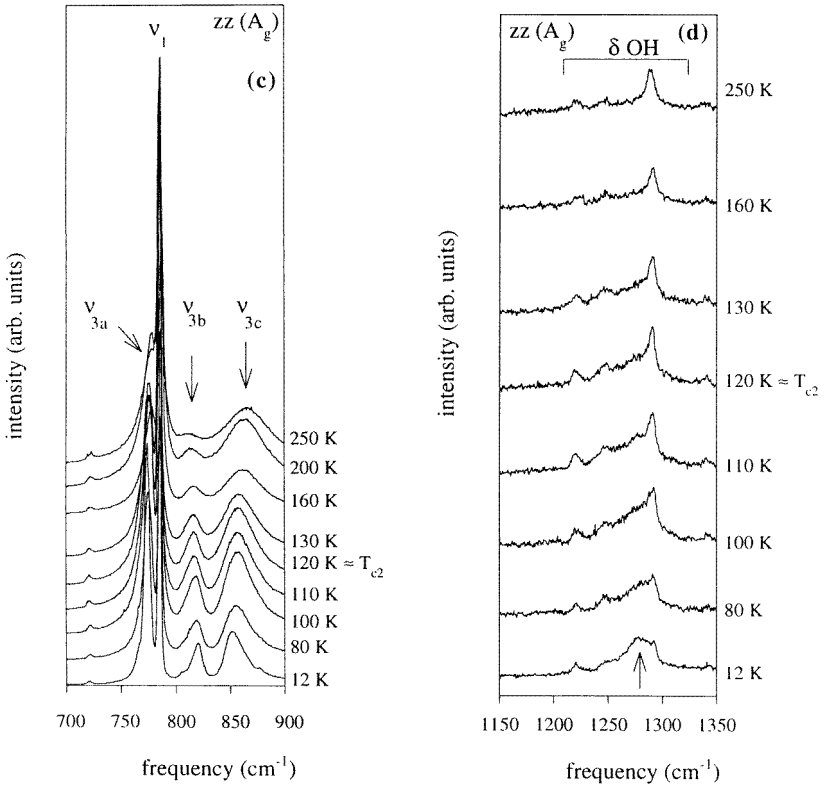

Figure 9. (Continued)

dependence does not exhibit any anomaly at T_{c2}, and the difference in frequency between ν_{3b} and ν_{3c} decreases with decreasing temperature (figure 10) while the lowering of symmetry of the crystal could have led to an increase of such splitting. It is possible that this unusual behaviour is related to a significative asymmetric deformation of AsO_4^{3-}, owing to the rotation of the betaine molecule.

Figure 9(d) shows the zz Raman spectra of BA for different temperatures in the frequency range of the δOH modes. We observe that the profile of the δOH bands is sensitive to the ferroelectric phase transition and a new B_u mode appears at 1280 cm^{-1}, below 120 K. As this mode carries a permanent dipolar moment, this feature may be related to the ordering of the hydrogen bonds in the ferroelectric phase of BA.

4.2. Phase transition sequence in DBA_{92}

In DBA_{92}, the phase transition at 411 K may be described by the condensation of a B_{2g} mode and the order parameter of the phase transition at $T_{c2} = 165$ K has the symmetry A_u. At $T_{c3} = 132$ K, it undergoes a first order ferroelectric phase transition which brings DBA_{92} to the same structure as the low temperature phase of BA. One can thus expect that some B_u modes of the paraelectric phase which triggered the transition in BA still play a role here. For this reason the phase sequence in DBA_{92} is best studied by recording the A_g low frequency spectra as a function of the temperature.

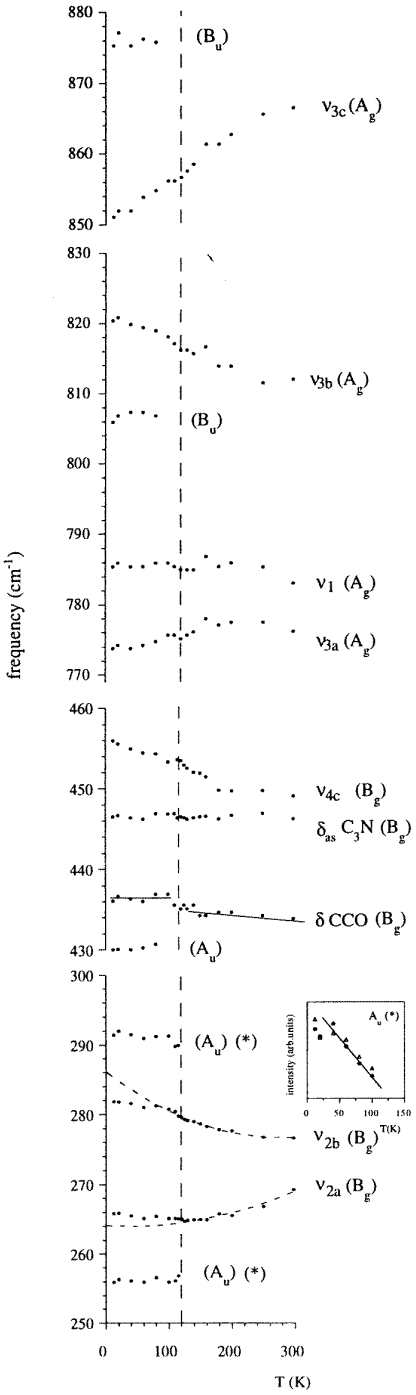

Figure 10. Vibration mode frequencies in BA versus temperature (12–300 K), in the region of the bending and stretching modes of the arsenate ion. The insert shows the intensities of the new ν_2 A_u modes as a function of the temperature. The dashed lines for $T < T_{c2}$ depict the qualitative extrapolations of the Debye lattice anharmonic contributions. The solid lines are guide lines.

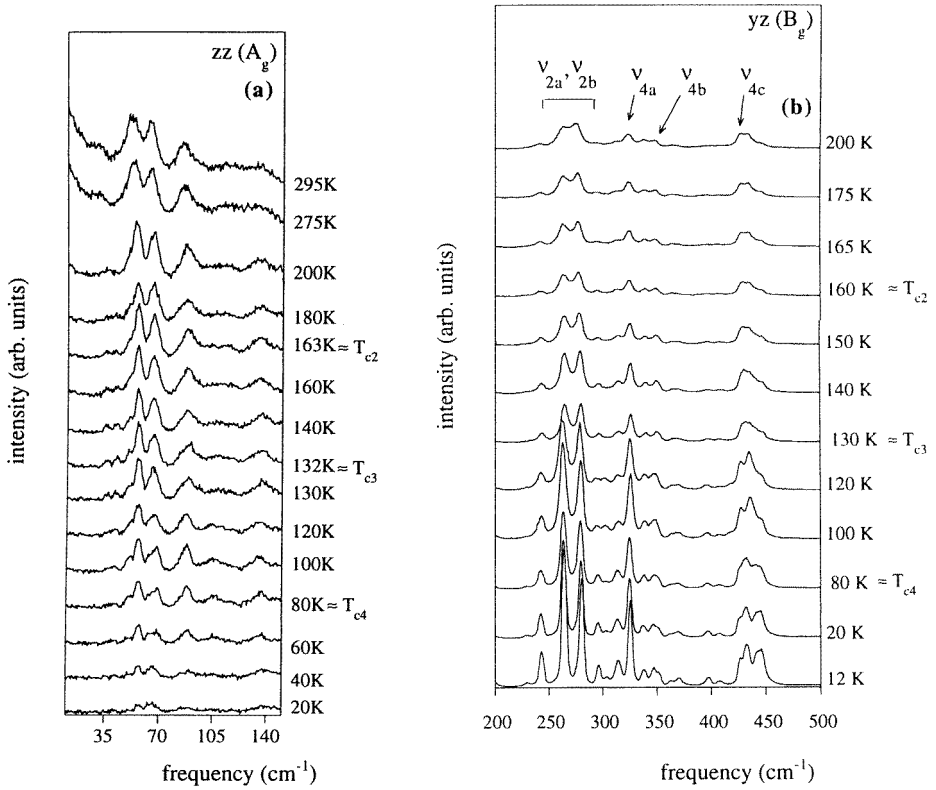

Figure 11. The Raman spectra for DBA_{92} for different temperatures in the frequency range: (a) 5 cm^{-1}–150 cm^{-1}; (b) 200 cm^{-1}–500 cm^{-1}; (c) 700 cm^{-1}–900 cm^{-1}; (d) 1150 cm^{-1}–1350 cm^{-1}.

The A_g external modes for the *zz* geometry can be seen in figure 11(a). There is no evidence for the existence of a soft mode in the vicinity of T_{c2} and no significative changes in the half-widths of the bands below that temperature are found. The low frequency A_g spectra give no clear indication about the character of the phase transitions of DBA_{92}.

As in BA, the most interesting features concern the behaviour of the internal modes of the AsO_4^{3-} ions. The spectra of these modes and their temperature dependence are displayed in the figures 11(b), (c) and 12, respectively.

The ν_1 mode presents the signature of the para–AF transition at T_{c2} but does not display any anomaly at the AFE–FE1 transition: there is a weak temperature dependence of its frequency above T_{c2} (see figure 12) which disappears below.

As was mentioned above, the ν_2 type modes are very sensitive to the ordering of protons or deuterons. In fact, very explicit anomalies are observed at T_{c2} for $\nu_{2b}(T)$ and at T_{c3} for $\nu_{2a}(T)$ (figure 12). By taking in account the different behaviour observed on these modes, it seems plausible that the two types of hydrogen bond, one mainly oriented along the *c*-axis and the other oriented in the *ab*-plane, become ordered at different temperatures. In agreement with this result, the two types of bond would play different roles in the mechanisms underlying the phase transitions observed in DBA_{92}. This assertion is supported by the fact that the onset of the FE1 phase does not correspond to the reversal of the polarization in one of the sub-lattices of the AFE phase [14].

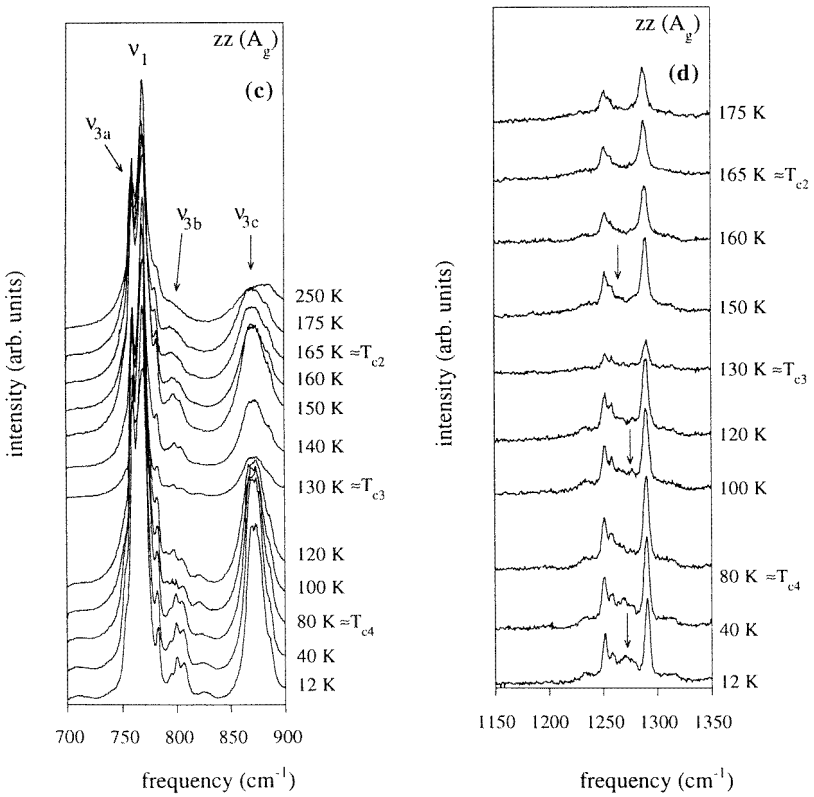

Figure 11. (Continued)

It is rather interesting to note that $\nu_{2b}(T)$ behaves in a similar way in DBA_{92} and in BA, displaying a change of slope at $T_{c2} = 163$ K and 119 K, respectively. This may suggest that a similar ordering mechanism of the hydrogen bonds takes place at T_{c2} in BA and DBA_{92}. We note also that the difference of frequencies between the dashed lines and the experimental data for a chosen temperature is more pronounced in DBA_{92} than in BA, due to the heavier mass of deuteron, which corroborates the interpretation we have given for to the anomalous change of slope in $\nu_{2b}(T)$.

The ν_4 modes exhibit definite, but very small changes of frequencies at T_{c2} and T_{c3}, much smaller than those which take place for BA. As far as the ν_3 modes are concerned, the difference with the BA case is again striking, for ν_{3b} and ν_{3c} which had a large variation with temperature in BA. This variation is particularly suppressed in DBA_{92}, replaced by a small splitting into two modes at T_{c3} for ν_{3c}, a larger splitting taking place at T_{c2} for ν_2. The ν_{3a} mode which already exhibited a small change of frequency in BA, has a still smaller one in DBA_{92}. Finally, the signature of the FE1–FE2 at T_{c4} transition can be mostly found in the behaviour of the ν_{4c}, AsO_4^{3-} mode, the $\delta_{as}C_3N$ and δCCO betaine modes.

Some additional modes appear at the FE1–FE2 phase transition which has been reported to be an isostructural one [4]. So, the breaking of symmetry responsible for this behaviour must be due to some local disorder.

The spectra of the δOH bending modes for DBA_{92} is seen in the 1150–1350 cm^{-1} frequency range for different temperatures (figure 11(d)). As is the case of BA, there is a

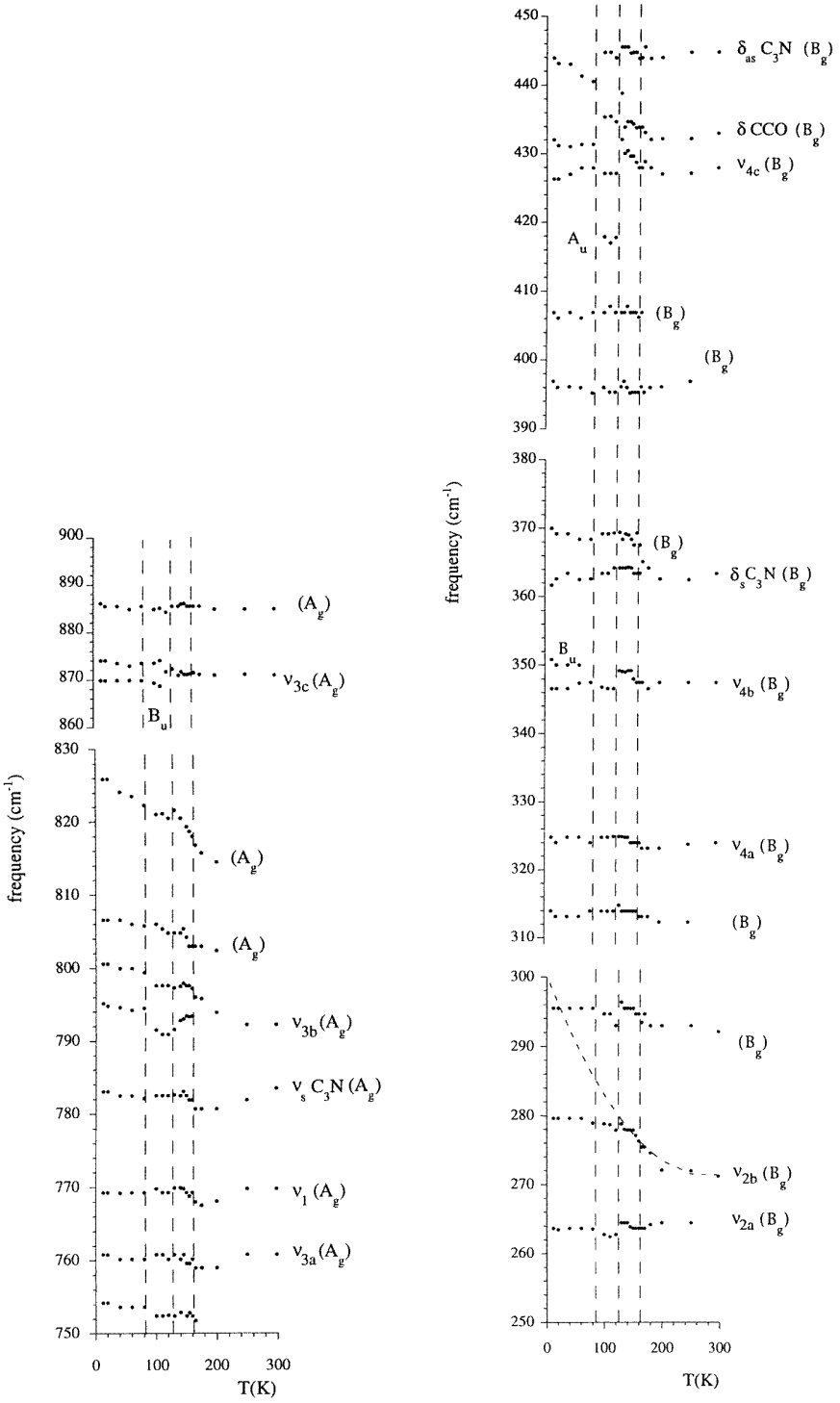

Figure 12. Vibration mode frequencies in DBA_{92} versus temperature (12–300 K), in the region of the bending and stretching modes of the arsenate ion. The dashed lines for $T < T_{c2}$ depict the qualitative extrapolations of the Debye lattice anharmonic contributions.

change in the profile of these bands with decreasing temperature and the appearance of new A_u and B_u modes (arrows in figure 11(d)). This complex behaviour can also be related to the ordering of the protons in the hydrogen bonds.

5. Conclusions

In this work we have proposed a tentative assignment for the different modes detected by Raman spectroscopy study in BA and DBA_{92} and tried to elucidate, without much success, the origin of the phase transition which takes place at $T_{c2} = 199$ K in BA and 163 K in DBA_{92}. No soft mode could be detected in the A_g geometry, which is not in favour of a displacive type transition. Conversely, the appearance of new modes in some geometry with an intensity proportional to $T_c - T$ is more in favour of such a mechanism, than of pure order–disorder transition which is generally characterized by the disparition of modes made visible by disorder induced scattering.

The behaviour of the internal modes of the AsO_4^{3-} ion has clearly shown the important deformation of this unit when introduced in the betaine arsenate lattice, certainly due to the asymmetric position of the betaine molecule. Therefore, a non-negligible contribution to the polarization in the ac-plane is expected in the ferroelectric phases. In BA, the study of the internal modes $\nu_{2a}(T)$ and $\nu_{2b}(T)$ provided evidence for the ordering of protons and for the role played by protons in the reinforcement of the coupling between the betaine molecule and AsO_4^{3-} ion at the para–FE phase transition. In DBA_{92}, the study of the internal modes $\nu_{2a}(T)$ and $\nu_{2b}(T)$ pointed to the existence of two types of hydrogen bond related to the mechanisms underlying the phase transitions at T_{c2} and T_{c3}. At variance with KDP-family compounds, the behaviour of $\nu_{2a}(T)$ and $\nu_{2b}(T)$ modes in BA and in DBA_{92} is a clear manifestation of the complex mechanisms which reveal a strong coupling between the betaine molecule and the AsO_4^{3-} ion.

Finally, our data on DBA provide also evidence that, in our deuteration technique, not only the hydrogen bonds are deuterated but also some of the methyl radicals of the betaine molecule.

Acknowledgments

We are deeply indebted to Professor Robert M Pick for his valuable assistance and fruitful advice during the analysis of experimental results and the writing up of this manuscript. The main results presented in this work are owing to his guidance and useful help.

We thank gratefully to Dr J Albers for his collaboration in the study of betaine compounds. The authors thank A Costa for his technical assistance and L G Viera for his computational assistance. This work was supported by the project PRAXIS/2/2.1/FIS/26/94. J Agostinho Moreira thanks Projecto Praxis for his grant (DB/3192/94).

References

[1] Klöpperpieper A, Rother H J, Albers J and Ehses K H 1982 *Ferroelectr. Lett.* **44** 115
[2] Schildckamp W, Schäfer G and Spilker J 1984 *Z. Kristallogr.* **168** 187
[3] Hayase S, Koshiba T, Terauchi H, Maeda M and Suzuki I 1989 *Ferroelectrics* **96** 221
[4] Agostinho Moreira J 1998 Private communication
[5] Müser H E and Schell U 1984 *Ferroelectrics* **55** 279
[6] Freitag O, Brückner H J and Unruh H G 1985 *Z. Phys.* B **61** 75
[7] Almeida A, Carvalho P, Chaves M R and Azevedo J C 1988 *Ferroelectr. Lett.* **9** 107

[8] Maeda M 1988 *J. Phys. Soc. Japan* **57** 2162
[9] Almeida A, Carvalho P, Chaves M R, Pires A R, Müser H E and Klöpperpieper A 1990 *Ferroelectrics* **108** 347
[10] Lacerda-Aroso M T, Ribeiro J L, Chaves M R, Almeida A, Vieira L G, Klöpperpieper A and Albers J 1994 *Phys. Status Solidi* b **185** 265
[11] Rother H J, Albers J, Klöpperpieper A and Müser H R 1985 *Japan. J. Appl. Phys.* **24** (Supplement 24-2) 384
[12] Schell U and Müser H E 1987 *Z. Phys.* B **66** 237
[13] Albers J, Klöpperpieper A, Müser H E and Rother H J 1984 *Ferroelectrics* **54** 45
[14] Almeida A, Simeão Carvalho P, Chaves M R, Klöpperpieper A and Albers J 1994 *Phys. Status Solidi* b **184** 225
[15] Balashova E V, Lemanov V V, Tagantsev A K, Sherman A B and Shomuradov Sh H 1995 *Phys. Rev.* B **51** 8747
[16] Brückner H J 1989 *Z. Phys.* B **75** 259
[17] Almeida A, Agostinho Moreira J, Chaves M R, Klöpperpieper A and Pinto F 1998 *J. Phys.: Condens. Matter* **10** 3035
[18] Pöppl A and Völkel G 1993 *Chem. Phys.* **171** 387
[19] Pöppl A, Völkel G, Tober O, Klöpperpieper A, Hüttermann J and Gatzweiler W 1993 *Chem. Phys.* **171** 375
[20] Suzuki I and Ohta N 1989 *Ferroelectrics* **96** 225
[21] Ouafik Z, Le Calvé N and Pasquier B 1995 *Chem. Phys.* **194** 145
[22] Farmer V C 1974 *The Infrared Spectra of Minerals* (London: Mineralogical Society)
[23] Ichikawa M 1978 *Acta. Crystallogr.* B **34** 2074
[24] Novak A 1974 *Struct. Bonding* **18** 177
[25] Sokolov N D, Vener M V and Savl'ev V A 1990 *J. Mol. Struct.* **222** 265
[26] Ouafik Z 1995 *PhD Thesis* Université Paris 6
[27] *Handbook of Chemistry and Physic* 70th edn (Boca Raton, FL: Chemical Rubber Company)
[28] Ehses K H and Spilker J 1990 *Ferroelektrizität '89, Kongress-Und Tagungsberichte der MLU (Halle-Wittenberg, 1990)*
[29] Courtens E and Vogt H 1985 *J. Chem. Physique* **82** 317